J Mol Model (2015) 21: 7
DOI 10.1007/s00894-014-2546-4

ORIGINAL PAPER

Binuclear cyclopentadienylrhenium hydride chemistry: terminal versus bridging hydride and cyclopentadienyl ligands

Xiaozhen Gao · Nan Li · R. Bruce King · Henry F. Schaefer III

Received: 20 September 2014 / Accepted: 24 November 2014 / Published online: 22 January 2015

Abstract Theoretical studies predict the lowest energy structures of the binuclear cyclopentadienylrhenium hydrides $Cp_2Re_2H_n$ (Cp = η^5–C_5H_5; n=4, 6, 8) to have a central doubly bridged $Re_2(\mu\text{–}H)_2$ unit with terminal η^5–Cp rings and the remaining hydrides as terminal ligands. However, the lowest energy $Cp_2Re_2H_2$ structure by more than 12 kcal mol^{-1} has one terminal η^5-Cp ring, a bridging η^3,η^2–Cp ring, and two terminal hydride ligands bonded to the same Re atom. The lowest energy hydride-free Cp_2Re_2 structure is a perpendicular structure with two bridging η^3,η^2–Cp rings. The previously predicted bent singlet Cp_2Re_2 structure with terminal η^5-Cp rings and a formal Re–Re sextuple bond lies ~37 kcal mol^{-1} above this lowest energy $(\eta^3,\eta^2\text{–Cp})_2Re_2$ structure. The thermochemistry of the $CpReH_n$ and $Cp_2Re_2H_n$ systems is consistent with the reported synthesis of the permethylated derivatives Cp^*ReH_6 and $Cp^*_2Re_2H_6$ (Cp^* = η^5–Me_5C_5) as very stable compounds. Additionally, natural bond orbital analysis, atoms-in-molecules and overlap population density-of-state in AOMIX were applied to present the existence of rhenium–rhenium multiple bonds.

Keywords Binuclear rhenium hydrides · Thermochemistry · Density functional theory

Electronic supplementary material The online version of this article (doi:10.1007/s00894-014-2546-4) contains supplementary material, which is available to authorized users.

X. Gao · N. Li (✉)
School of Mechatronical Engineering,
Beijing Institute of Technology, Beijing 100081, China
e-mail: leen04@163.com

R. B. King (✉) · H. F. Schaefer III
Department of Chemistry and Center for Computational Chemistry,
University of Georgia, Cedar Street, Athens, Georgia 30602, USA
e-mail: rbking@chem.uga.edu

X. Gao · N. Li
State Key Laboratory of Explosion Science and Technology, Beijing Institute of Technology, Beijing 100081, People's Republic of China

Introduction

A characteristic feature of rhenium chemistry is the facility with which it forms stable hydride derivatives. The first hydride of rhenium was actually prepared shortly after the discovery of rhenium but not recognized as such for many years. Thus, an early attempt to generate a lower rhenium oxidation state by the reduction of acid solutions of perrhenate with zinc amalgam gave what was initially believed to be "potassium rhenide" analogous to potassium chloride with rhenium in the −1 oxidation state [1]. However, this reduction product was eventually shown by neutron diffraction to be K_2ReH_9 with an unusual nine-coordinate anion with nine Re–H bonds [2]. Also in the development of metallocene chemistry, the yellow sublimable solid obtained from sodium cyclopentadienide and rhenium pentachloride was not a parallel rhenocene sandwich compound analogous to ferrocene but instead the hydride Cp_2ReH (Cp = η^5–C_5H_5) with tilted planar Cp rings [3].

The use of pentamethylcyclopentadienyl (Cp*) rather than unsubstituted cyclopentadienyl as a ligand has allowed the development of extensive chemistry of pentamethylcyclopentadienyl rhenium hydride derivatives with a Cp*/Re ratio of 1:1. The stable compounds containing only Cp* and hydride ligands are the mononuclear [4, 5] Cp^*ReH_6 and the binuclear $Cp^*_2Re_2H_6$ (Fig. 1). In the binuclear hydride, two of the hydride ligands form bridges leaving two terminal hydrides for each rhenium atom.

In order to learn more about these cyclopentadienylrhenium hydride systems, we undertook a density functional theory (DFT) study using the unsubstituted Cp (= η^5–C_5H_5) rather than Cp* to facilitate the calculations. We report here our results with the mononuclear $CpReH_n$ (n=6, 4, 2) and the binuclear $Cp_2Re_2H_n$ (n=8, 6, 4, 2) systems as well as the hydride-free Cp_2Re_2 system. The binuclear $Cp_2Re_2H_n$ systems are of interest because of the relative stabilities of various

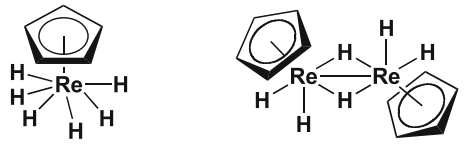

$(\eta^5\text{-}Me_5C_5)ReH_6$ $(\eta^5\text{-}Me_5C_5)_2Re_2(\mu\text{-}H)_2H_4$

Fig. 1 Structures of the known Cp^*ReH_6 and $Cp^*_2Re_2H_6$ (= $Cp^*_2Re_2(\mu\text{-}H)_2H_4$). Ring methyl groups are omitted for clarity

structures with bridging and/or terminal Cp rings and bridging and/or terminal hydride ligands. Hydride-free Cp_2Re_2 structures with terminal Cp rings were previously studied in order to identify structures with apparent high-order rhenium-rhenium multiple bonds [7]. At that time singlet and triplet Cp_2Re_2 structures with terminal Cp rings were identified that were suggested by their frontier molecular orbitals and ultrashort Re–Re distances to have formal sextuple and quintuple Re–Re bonds, respectively. However, we now find that the lowest energy such structure lies more than 35 kcal mol^{-1} in energy above the lowest energy perpendicular $Re_2(\mu\text{–}Cp)_2$ structure with two bridging Cp rings. Thus we suspect that the Cp_2Re_2 structures discussed in the earlier paper [7] are not likely to be realizable experimentally.

Theoretical methods

All calculations were performed using the Gaussian 09 program package [8]. Two density functional theory (DFT) methods were used in this study. One is the BP86 method, which is a pure DFT method combining Becke's 1988 exchange functional with Perdew's 1986 correlation functional [9, 10]. The other is the MPW1PW91 method [11], which is a so-called second generation functional [12], combining the modified Perdew-Wang exchange functional with the Perdew-Wang's 1991 correlation functional [13]. The MPW1PW91 method has been found to be typically more suitable for geometry optimization of the second and third row transition metal systems [14, 15], while the BP86 method usually provides better vibrational frequencies.

For the third row transition metals, the large numbers of electrons increase exponentially the computational effort required. In order to reduce such efforts and the resulting cost, effective core potential (ECP) relativistic basis sets were employed. Thus the SDD (Stuttgart-Dresden ECP plus DZ) basis set [16] was used for Re atoms. For C atoms, one set of pure spherical harmonic d functions with orbital exponent $\alpha_d(C)=0.75$, was added to the Huzinaga-Dunning standard contracted DZ sets, designated as (9s5p1d/4s2p1d) [17, 18]. For H atoms, a set of p polarization functions [α_p (H)=0.75] was added to the Huzinaga-Dunning DZ sets [19].

The geometries of all the structures were fully optimized using the two selected DFT methods with the basis sets indicated above. The harmonic vibrational frequencies were obtained at the same levels by evaluating analytically the second derivatives of the energy with respect to the nuclear coordinates. The fine grid (75, 302) was the default for evaluating integrals numerically [20]. The finer grid (120, 974) was used for more precise resolution of the small imaginary vibrational frequencies. The tight 10^{-8} Hartree designation is the default for the self-consistent field (SCF) convergence.

The optimized structures for $CpReH_n$ (n=2, 4, 6) and $Cp_2Re_2H_n$ (n=2, 4, 6, 8) are depicted in Figs. 2–7 in the Results. The binuclear derivatives are labeled as ***n*H–*x*X** where ***n*** is the number of H atoms, ***x*** is the rank of the structure in the order of relative energies, and **X** refers to the spin state with **S** and **T** corresponding to the singlet and triplet spin states, respectively. For example, the singlet energetically lowest-lying structure of $Cp_2Re_2H_2$ is designated as **2H-1S**. The bond distances in the figures were determined by the MPW1PW91 (upper) and BP86 (lower) methods, respectively. In this paper, the bond distances in structures $CpReH_6$ and $Cp_2Re_2H_6$ predicted by the MPW1PW91 method are greater than those predicted by BP86 method (experimental structures, see Tables 3 and 8 below). Thus, we discuss the vibrational frequencies by means of the BP86 method, and other results using the MPW1PW91 method.

The bonding characters of each species of Re–Re bonds are discussed in terms of natural bond orbitals (NBO) [21, 22] in

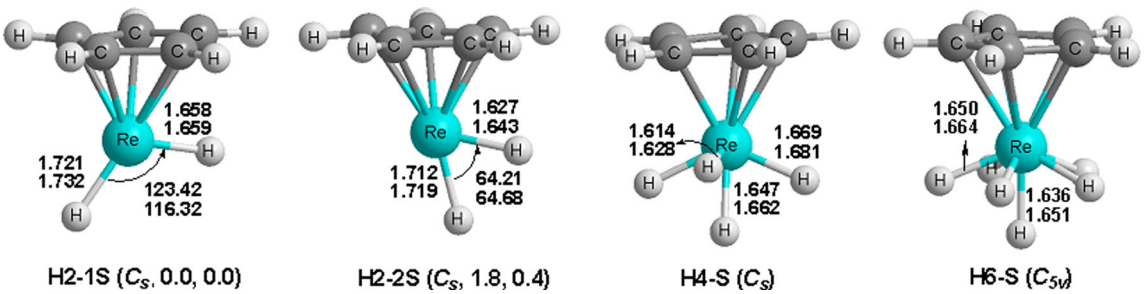

Fig. 2 Optimized geometries (bond lengths in Å) at the MPW1PW91/DZP (*upper values*) and BP86/DZP (*lower values*) levels of theory for the four singlet state $CpReH_n$ structures (n=2, 4, 6). The numbers in parentheses are the relative energies (ΔE in kcal mol^{-1} predicted by the MPW1PW91 and BP86 methods, respectively). Subsequent figures have the same arrangement

the program package GenNBO and atoms-in-molecules (AIM) [23]. The NBO method can transform the confusing delocalized molecular orbitals into canonical molecular orbitals (CMO); the CMO module provides a capsule description of the NBO composition of each CMO (occupied and virtual) as well as the percentage bonding, nonbonding, or antibonding characters of each MO. The AOMiX [24, 25] package was also explored to predict the quadruple bond between the Re atoms in **4H-8S** that is predicted at the MPW1PW91/DZP level of theory.

Results

Structures for CpReHn (n=2, 4, 6)

Four structures were optimized for the mononuclear rhenium derivatives $CpReH_n$ (n=2, 4, 6) (Fig. 2). Total and relative energies, number of imaginary vibrational frequencies and Re–H bond distances for the four singlet state structures are given in Table 1. The singlet $CpReH_6$ structure **H6-S** has C_{5v} symmetry with a terminal η^5–Cp ring, five symmetry equivalent terminal hydrogen atoms and a sixth unique terminal hydrogen atom. The infrared-active ν(Re–H) frequencies in **H6-S** of 2066, 2076, and 2147 cm^{-1} predicted by the BP86 method (Table 2), are somewhat higher than the experimentally observed ν(Re–H) frequency of 2018 cm^{-1} observed in $(C_5Me_5)ReH_6$ [4]. The Re–H distances in **H6-S** of 1.636 and 1.650 Å (MPW1PW91) or 1.651 and 1.664 Å (BP86) (Table 3) are close to the experimental Re–H distances of 1.66(5) Å in $(\eta^5\text{-}C_5Me_5)ReH_6$ as estimated by NMR [5]. This could be an effect of the methyl substituents on the Cp ring.

The singlet $CpReH_4$ structure **H4-S** has C_s symmetry with one terminal η^5–Cp ring and four terminal hydrogen atoms (Fig. 2). Two of the hydrogen atoms are located in the mirror plane whereas the other two hydrogen atoms are related by mirror plane reflection. Structure **H4-S** can be derived from the $CpReH_6$ structure **H6-S** by removal of a pair of symmetry-related hydrogen atoms. In **H4-S** the terminal Re–H distance derived from the unique hydrogen atom in **H6-S** is 1.647 Å (MPW1PW91) or 1.662 Å (BP86) whereas the other Re–H distances are 1.614 Å (MPW1PW91) or 1.628 Å (BP86) and 1.669 Å (MPW1PW91) or 1.681 Å (BP86).

Two $CpReH_2$ structures were optimized lying within ~2 kcal mol^{-1} of energy (Fig. 2). The slightly lower energy structure **H2-1S** is predicted to be a C_s structure with one terminal η^5–Cp ring and two terminal H hydrogen atoms. The Re–H distances are 1.721 Å (MPW1PW91) or 1.732 Å (BP86) and 1.658 Å (MPW1PW91) or 1.659 Å (BP86). The H–Re–H angle in **H2-1S** is an obtuse angle of 123.4° (MPW1PW91) or 116.3° (BP86). The other $CpReH_2$ structure **H2-2S** is also a C_s structure lying only 1.8 kcal mol^{-1} (MPW1PW91) or 0.4 kcal mol^{-1} (BP86) above **H2-1S**. The geometry of **H2-2S** is similar to that of **H2-1S** except for the acute H–Re–H angle of 64.2° (MPW1PW91) or 64.7° (BP86) as compared with the obtuse H–Re–H angle in **H2-1S**. The Re–H distances in **H2-2S** of 1.712 and 1.627 Å (MPW1PW91) or 1.719 and 1.643 Å (BP86) are shorter than those in **H2-1S**.

Structures for $Cp_2Re_2H_n$ (n=8, 6, 4, 2)

$Cp_2Re_2H_8$ structures

Three singlet state low energy $Cp_2Re_2H_8$ structures were found (Fig. 3; Tables 4 and 5). Each structure has two terminal η^5–Cp rings. The global minimum $Cp_2Re_2H_8$ structure **8H-1S** is a bent C_{2h} structure with two bridging hydrogen atoms and six terminal hydrogen atoms with three of the latter bonded to each Re atom. The bridging Re–H distances are 1.849 Å (MPW1PW91) or 1.863 Å (BP86) whereas the terminal Re–H distances are significantly shorter at 1.640 and 1.636 Å (MPW1PW91) or 1.654 Å and 1.648 Å (BP86). The predicted doubly H-bridged Re–Re distance of 2.769 Å (MPW1PW91) or 2.773 Å (BP86) in **8H-1S** is close to the experimental Re–Re distances of 2.69 Å and 2.72 Å in $Cp^*Re_2OCl_2(\mu\text{–}O)_2$ and $Cp^*Re_2Cl_4(\mu\text{–}O)_2$ [26], respectively. Natural bond orbital (NBO) analysis indicates no direct Re···Re bond in this isomer. Thus, the structure **8H-1S** is an unsaturated structure.

Table 1 Total energies (E, in Hartree), relative energies (ΔE, in kcal mol^{-1}), number of imaginary vibrational frequencies (Nimag) and Re–H bond distance (Å) for the four singlet state structures of $CpReH_n$ (n=2, 4, 6)

		H2-1S (C_s)	H2-2S (C_s)	H4-S (C_s)	H6-S (C_{5v})
MPW1PW91	E	−272.862990	−272.860179	−274.090097	−275.320194
	ΔE	0.0	1.8	0.0	0.0
	Nimag	0	0	0	0
	Re-H	1.658,1.659	1.712,1.627	1.614,1.647,1.669	1.636,1.650
BP86	E	−273.000544	−272.999898	−274.231622	−275.465618
	ΔE	0.0	0.4	0.0	0.0
	Nimag	0	0	0	0
	Re-H	1.721,1.732	1.719,1.643	1.628,1.662,1.681	1.651,1.664

Table 2 ν(Re–H) frequencies (cm^{-1}) and infra-red (IR) intensities (km mol^{-1}) for the four $CpReH_n$ (n=2, 4, 6) structures and the experimental ν(Re–H) frequencies (cm^{-1}) of $(C_5Me_5)ReH_6$

	BP86
H2-1S (C_s)	1903(248), 2060(49)
H2-2S (C_s)	1929(135), 2110(5)
H4-S (C_s)	1985(98), 2012(71), 2106(46), 2183(7)
H6-S (C_{5v})	2066(37), 2066(37), 2076(24), 2077(0), 2077(0), 2147(24)
$(C_5Me_5)ReH_6$[a]	2018

[a] Experimental value from ref [4]

The next singlet spin state structure for $Cp_2Re_2H_8$ is **8H-2S**, lying 7.7 kcal mol^{-1} (MPW1PW91) or 7.9 kcal mol^{-1} (BP86) in energy above the global minimum structure **8H-1S** (Fig. 3; Tables 4 and 5). Structure **8H-2S** is geometrically similar to **8H-1S**, except for the *cis* rather than *trans* orientation of the Cp rings. In **8H-2S**, the bridging Re–H distances are 1.851 Å (MPW1PW91) or 1.865 Å (BP86) whereas the terminal Re–H distances are 1.636 and 1.632 Å (MPW1PW91) or 1.650 and 1.646 Å (BP86). The predicted doubly H-bridged Re–Re distance is 2.839 Å (MPW1PW91) or 2.856 Å (BP86) in **8H-2S**. NBO analysis indicates no direct Re···Re bond in **8H-2S**. Thus, structure **8H-2S** is also an unsaturated structure. The bridging hydrogen atoms in **8H-1S** and **8H-2S** exhibit ν(Re–H) frequencies around 1200 cm^{-1} whereas the terminal ν(Re–H) frequencies range from 2087 to 2174 cm^{-1} (Table 5).

The third $Cp_2Re_2H_8$ structure **8H-3S**, lying 15.7 kcal mol^{-1} (MPW1PW91) or 8.2 kcal mol^{-1} (BP86) in energy above the lowest energy structure **8H-1S**, is predicted to be a C_{2h} structure with all terminal hydrogen atoms and a *trans* orientation of the Cp rings (Fig. 3, Table 4). Each rhenium bonds to four terminal H hydrogen atoms. The predicted terminal Re–H distances are 1.639, 1.616, and 1.648 Å (MPW1PW91) or 1.654, 1.632, and 1.662 Å (BP86). The predicted Re–Re distance of 2.580 Å (MPW1PW91) or 2.601 Å (BP86) in **8H-3S** is ~0.2 Å less than that in **8H-1S**. According to the NBO analysis, there is an unbridged formal Re=Re double bond in **8H-3S**. This gives each rhenium atom in **8H-3S** the favored 18-electron configuration.

$Cp_2Re_2H_6$ structures

Four energetically singlet state lower-lying structures were found for $Cp_2Re_2H_6$ (Fig. 4; Tables 6 and 7). The isomers with one terminal H atom on each Re atom and three or four bridging [27–31] H atoms were considered for $Cp_2Re_2H_6$. For example, the predicted isomer with one terminal H atom on each Re atom and four bridging H atoms has three imaginary frequencies (−389i cm^{-1}, −134i cm^{-1}, −46i cm^{-1}) indicating the absence of the stationary points with this structure. Ultimately, structure **6H-1S** will be favored. The global minimum structure **6H-1S** is predicted to be a C_{2h} structure with a *trans* orientation of two terminal η^5-Cp rings, two terminal hydrogen atoms bonded to each Re atom, and two bridging H hydrogen atoms. The terminal Re–H distance is 1.650 Å (MPW1PW91) or 1.665 Å (BP86), and the bridging Re–H distance is 1.796 Å (MPW1PW91) or 1.812 Å (BP86). The predicted Re–Re distance of 2.450 Å (MPW1PW91) or 2.460 Å (BP86), which is close to the experiment Re–Re bond length (Table 8), is ~0.3 Å less than that in the $Cp_2Re_2H_8$ structure **8H-1S**. NBO analysis found a Re–Re single bond in **6H-1S**. According to the NBO

Table 3 The predicted structures of the $CpReH_6$ compared with the known Cp^*ReH_6

H6-1S(C_{5v})	MPW1PW91	BP86	Exp [5]
Re-H (Å)	1.650	1.664	1.55(2),1.64(2),1.61(2),1.40(2),1.65(2) with the average 1.57(2)
Re-H(⊥Re) (Å)	1.636	1.651	1.662
Re-Cp (or Cp*) (Å)	1.973	1.996	1.951
Re-C (Å)	2.316	2.341	2.295(2),2.302(3),2.304(3),2.299(3),2.291(2) with the average 2.298(2)
C-C (Å)	1.427	1.438	1.424(4),1.437(4),1.446(4),1.420(3),1.427(3) with the average 1.431(1)
Cp(or Cp*)-Re-H (°)	112.45	112.40	114, 109, 110, 111,113, with the average 111.4
Cp(or Cp*)-Re-H(⊥Re) (°)	180.00	180.00	174
H-Re-H (°)	65.81	65.84	76(1), 61(1), 52(1), 54(1), with the average 66.2

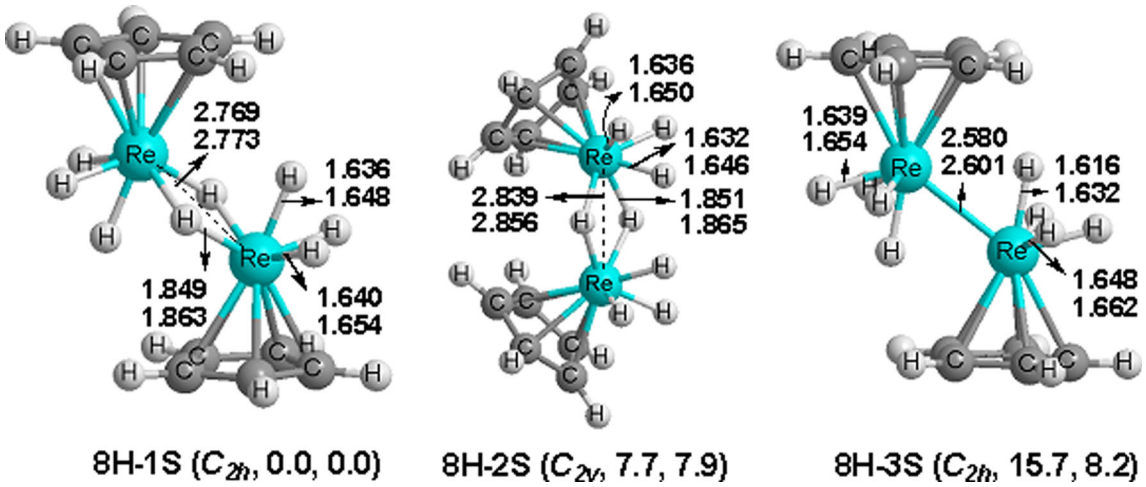

Fig. 3 The three singlet state stationary points of $Cp_2Re_2H_8$

results, structure **6H-1S** is also an unsaturated structure. The next $Cp_2Re_2H_6$ structure **6H-2S**, lying only 1.7 kcal mol^{-1} (MPW1PW91) or 1.8 kcal mol^{-1} (BP86) in energy above **6H-1S**, is similar to **6H-1S** except for a *cis* rather than *trans* orientation of the two Cp rings. The bridging ν(Re–H) frequencies in **6H-1S** and **6H-2S** are approximately 1620 cm^{-1} whereas the terminal ν(Re–H) frequencies range from 2050 to 2068 cm^{-1}.

The next singlet $Cp_2Re_2H_6$ structure **6H-3S**, lying 14.2 kcal mol^{-1} (MPW1PW91) or 7.3 kcal mol^{-1} (BP86) in energy above **6H-1S**, is predicted to have C_{2h} symmetry with two terminal η^5-Cp rings in a *trans* orientation and three terminal hydrogen atoms on each Re atom (Fig. 4; Tables 6 and 7). Structure **6H-3S** has a small imaginary vibrational frequency of 21i cm^{-1} (MPW1PW91) or 22i cm^{-1} (BP86), which can be removed using the finer (120, 974) integration grid. The terminal Re–H distances in **6H-3S** are 1.649 Å (MPW1PW91) or 1.663 Å (BP86) and 1.657 Å (MPW1PW91) or 1.673 Å (BP86). NBO analysis indicates the existence of the triple Re≡Re bond giving the two Re atoms a favored 18-electron configuration. The unbridged Re≡Re distance of 2.291 Å (MPW1PW91) or 2.312 Å (BP86) in **6H-3S** is ~0.3 Å shorter than the Re=Re double bond distance in **8H-3S**. This leads to the favored 18-electron configuration for each Re atom in **6H-3S**. The last low-energy singlet $Cp_2Re_2H_6$ structure **6H-4S**, lying 14.3 kcal mol^{-1} (MPW1PW91) or 7.8 kcal mol^{-1} (BP86) in energy above **6H-1S**, is geometrically similar to **6H-3S** except for a *cis* rather than *trans* orientation of the Cp rings.

Table 4 Total energies (*E*, in Hartree), relative energies (Δ*E*, in kcal mol^{-1}), and Re–Re bond distances (Å) for the three singlet state $Cp_2Re_2H_8$ structures. None of the structures has any imaginary vibrational frequencies

		8H-1S(C_{2h})	8H-2S(C_{2v})	8H-3S(C_{2h})
MPW1PW91	*E*	−548.290958	−548.278680	−548.265981
	Δ*E*	0.0	7.7	15.7
	Nimag	0	0	0
	Re-Re	2.769	2.839	2.580
BP86	*E*	−548.570353	−548.557694	−548.557332
	Δ*E*	0.0	7.9	8.2
	Nimag	0	0	0
	Re-Re	2.773	2.856	2.601

$Cp_2Re_2H_4$ structures

Eight singlet state energetically lower-lying structures were found for $Cp_2Re_2H_4$ (Fig. 5; Tables 9 and 10). The global minimum $Cp_2Re_2H_4$ structure is the C_i structure **4H-1S** with two terminal η^5-Cp rings in a *trans* orientation, two bridging hydrogen atoms, and a single terminal hydrogen atom on each Re atom. The Re–H distances to the terminal hydrogen atoms are 1.656 Å (MPW1PW91) or 1.672 Å (BP86). The bridging Re–H distances are 1.877 Å (MPW1PW91) or 1.878 Å (BP86) and 1.733 Å (MPW1PW91) or 1.751 Å (BP86). The

Table 5 ν(Re-H) frequencies and IR intensities (km mol^{-1}) for the three $Cp_2Re_2H_8$ structures

	BP86
8H-1S(C_{2h})	1188(0)[a], 1212(33)[a], 2087(0), 2089(36), 2104(98), 2104(0), 2162(0), 2165(71)
8H-2S(C_{2v})	1223(0)[a], 1244(260)[a], 2100(21), 2101(0), 2109(2), 2114(68), 2139(30), 2174(8)
8H-3S(C_{2h})	2069(0), 2070(50), 2073(76), 2074(0), 2075(31), 2082(0), 2264(26), 2268(0)

[a] Bridging ν(Re-H) frequencies

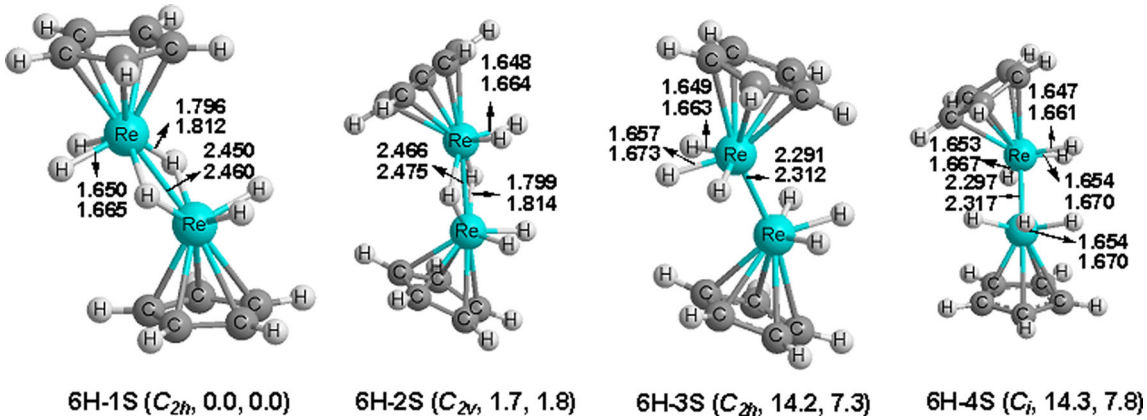

Fig. 4 The four singlet state stationary points of $Cp_2Re_2H_6$

predicted doubly H-bridged Re–Re distance in **4H-1S** is 2.418 Å (MPW1PW91) or 2.426 Å (BP86). NBO analysis indicates a double Re=Re bond in **4H-1S**. Structure **4H-5S** is similar to structure **4H-1S** except for a *cis* orientation of the η^5-Cp rings.

The second singlet $Cp_2Re_2H_4$ structure **4H-2S**, lying 3.4 kcal mol^{-1} (MPW1PW91) or 5.5 kcal mol^{-1} (BP86) in energy above **4H-1S**, is predicted to be a C_i coaxial structure with two terminal η^5-Cp rings and four bridging hydrogen atoms (Fig. 5; Tables 9 and 10). Structure **4H-2S** has a small imaginary vibrational frequency of 22i cm^{-1} (MPW1PW91) or 12i cm^{-1} (BP86), which can be removed using the finer (120, 974) integration grid, indicating that this small imaginary frequency arises from numerical integration error [32]. The bridging Re–H distances connecting to the "upper" Re atom (Fig. 5) are 1.822 Å (MPW1PW91) or 1.825 Å (BP86) and 1.850 Å (MPW1PW91) or 1.865 Å (BP86), and those connecting to the "lower" Re atom are 1.836 Å (MPW1PW91) or 1.852 Å (BP86) and 1.864 Å (MPW1PW91) or 1.893 Å (BP86). The predicted Re–Re distance is 2.416 Å (MPW1PW91) or 2.442 Å (BP86). The NBO analysis indicates just a single σ (d_z^2–d_z^2) bond in **4H-2S**. It is worth mentioning that theoretical calculations by Suzuki [33–35] on the diruthenium compound suggested that there was no metal–metal bond in this species including $Cp_2Ru_2H_4$ and $Cp_2Fe_2H_4$. Structure **4H-2S** is a rare example of a tetrabridged structure that is a low-energy genuine minimum.

The next singlet $Cp_2Re_2H_4$ structure **4H-3S**, lying 4.0 kcal mol^{-1} (MPW1PW91) or 4.3 kcal mol^{-1} (BP86) in energy above **4H-1S**, is predicted to be a C_1 structure with two terminal η^5-Cp rings in a *cis* orientation, one bridging hydrogen atom, and three terminal hydrogen atoms (Fig. 5; Tables 9 and 10). The bridging Re–H distances are 1.840 and 1.799 Å (MPW1PW91) or 1.836 and 1.830 Å (BP86). The terminal Re–H distances are significantly shorter at 1.648 and 1.654 Å (MPW1PW91) or 1.664 and 1.671 Å (BP86) to the ReH_2 moiety and 1.661 Å (MPW1PW91) or 1.674 Å (BP86) to the ReH moiety. The short predicted Re–Re distance is 2.386 Å (MPW1PW91) or 2.370 Å (BP86). NBO analysis indicates a double bond between the two Re atoms. The next singlet $Cp_2Re_2H_4$ structure **4H-4S**, lying 5.5 kcal mol^{-1} (MPW1PW91) or 4.3 kcal mol^{-1} (BP86) in energy above **4H-1S**, is geometrically similar to **4H-3S** except the η^5-Cp rings are in a *trans* orientation rather than a *cis* orientation.

The next $Cp_2Re_2H_4$ structure **4H-6S**, lying 8.1 kcal mol^{-1} (MPW1PW91) or 11.0 kcal mol^{-1} (BP86) above **4H-1S**, is an

Table 6 Total energies (E, in hartree), relative energies (ΔE, in kcal mol^{-1}), numbers of imaginary vibrational frequencies (Nimag), and Re–Re distances (Å) for the four singlet state structures of $Cp_2Re_2H_6$

		6H-1S(C_{2h})	6H-2S(C_{2v})	6H-3S(C_{2h})	6H-4S(C_2)
MPW1PW91	E	−547.132697	−547.130018	−547.110017	−547.109889
	ΔE	0.0	1.7	14.2	14.3
	Nimag	0	0	1(21i)[a]	0
	Re-Re	2.450	2.466	2.291	2.297
BP86	E	−547.414716	−547.411918	−547.403081	−547.402333
	ΔE	0.0	1.8	7.3	7.8
	Nimag	0	0	1(22i)[a]	0
	Re-Re	2.460	2.475	2.312	2.317

[a] Imaginary vibrational frequency diminishing after using grid (120974)

Table 7 ν(Re-H) frequencies and IR intensities (km mol^{-1}) for the four $Cp_2Re_2H_6$ structures

	BP86
6H-1S (C_{2h})	1623(1)[a], 1628(0)[a], 2050(33), 2051(89), 2054(0), 2058(0)
6H-2S (C_{2v})	1618(0)[a], 1625(1)[a], 2057(25), 2062(0), 2068(47), 2068(49)
6H-3S (C_{2h})	2028(96), 2032(0), 2058(34), 2059(0), 2061(9), 2068(0)
6H-4S (C_2)	2044(74), 2047(18), 2065(11), 2067(15), 2078(7), 2083(10)

[a] Bridging ν(Re-H) frequencies

unsymmetrical structure with two η^5-Cp rings in a *cis* orientation, two bridging hydrogen atoms and two terminal hydrogen atoms bonded to the same Re atom (Fig. 5; Tables 9 and 10). Structure **4H-6S** has a small imaginary frequency of 15i cm^{-1} by MPW1PW91, which can be removed using the finer (120, 974) integration grid. The BP86 method gives a small imaginary vibrational frequency of 24i cm^{-1}, which decreases to the negligible 1i cm^{-1} after using the finer (120, 974) grid. This indicates that this small imaginary frequency arises from numerical integration error. The bridging Re–H distances in **4H-6S** are 1.781 and 1.859 Å (MPW1PW91) or 1.785 and 1.895 Å (BP86). The terminal Re–H distances are 1.648 Å (MPW1PW91) or 1.663 Å (BP86). NBO analysis points out just a single bond between the two Re atoms with the predicted Re–Re distance of 2.444 Å (MPW1PW91) or 2.454 Å (BP86).

The next singlet $Cp_2Re_2H_4$ structure **4H-7S**, lying 11.2 kcal mol^{-1} (MPW1PW91) or 10.6 kcal mol^{-1} (BP86) in energy above **4H-1S**, is a C_1 structure with one terminal η^5-Cp ring, one bridging η^2,η^3-μ-Cp ring, two bridging hydrogen atoms, and two terminal hydrogen atoms bonded to the same Re atom (Fig. 5; Tables 9 and 10). The terminal Re–H distances connecting the "upper" Re atom are 1.67 Å (MPW1PW91) or 1.68 Å (BP86). In **4H-7S** the bridging Re–H distances connecting to the ReH_2 unit are 1.826 and 1.882 Å (MPW1PW91) or 1.909 and 1.946 Å (BP86) whereas the bridging Re–H distances connecting to the CpRe unit without terminal hydrogens are 1.783 and 1.845 Å (MPW1PW91) or 1.748 and 1.845 Å (BP86). The Re–Re distance is predicted to be 2.435 Å (MPW1PW91) or 2.444 Å (BP86). NBO analysis shows clearly a single bond between the two Re atoms.

The last low-energy singlet $Cp_2Re_2H_4$ structure **4H-8S**, lying 13.4 kcal mol^{-1} (MPW1PW91) or 3.5 kcal mol^{-1} (BP86) in energy above **4H-1S**, is a bent unbridged C_{2h} structure with two terminal η^5-Cp rings and two terminal H hydrogen atoms bonded to each Re atom (Fig. 5; Tables 9 and 10). The predicted terminal Re–H distances in **4H-8S** are 1.666 Å (MPW1PW91) or 1.679 Å (BP86). The very short Re–Re distance in **4H-8S** of 2.242 Å (MPW1PW91) or 2.257 Å (BP86) is similar to the experimental Re–Re unbridged quadruple bond distance of 2.24 Å in the dianion [36] $Re_2Cl_8^{2-}$ and thus is interpreted as a formal quadruple bond. At the same time, NBO analysis also suggests a quadruple bond between the two Re atoms. This gives each Re atom in **4H-8S** the favored 18-electron configuration.

$Cp_2Re_2H_2$ structures

Five singlet state low energy $Cp_2Re_2H_2$ structures were optimized (Fig. 6; Tables 11 and 12). The lowest energy of these structures is **2H-1S**, with a bridging η^2,η^2-Cp ring, one terminal η^5-Cp ring, and both of the terminal hydrogen atoms bonded to the same Re atom. The terminal Re–H distances in **2H-1S** are 1.635 and 1.700 Å (MPW1PW91) or 1.653 and 1.710 Å (BP86). The ultrashort Re–Re distance in **2H-1S** is 2.275 Å (MPW1PW91) or 2.296 Å (BP86).

Structure **2H-1S** appears to be a relatively favorable $Cp_2Re_2H_2$ structure since the next $Cp_2Re_2H_2$ structure in terms of relative energy, namely **2H-2S**, lies 12.5 kcal mol^{-1} (MPW1PW91) or 13.0 kcal mol^{-1} (BP86) above **2H-1S**. Structure **2H-2S** is a C_{2v} perpendicular structure with two bridging η^2,η^3-Cp rings and a terminal hydrogen atom bonded to each Re atom in a *cis* orientation (Fig. 6; Tables 11 and 12). The Re–H distances in **2H-2S** are 1.681 Å (MPW1PW91) or 1.697 Å (BP86). The short Re–Re distance of 2.247 Å (MPW1PW91) or 2.262 Å (BP86) can be regarded as a double bond between the two Re atoms suggested by the NBO analysis. The $Cp_2Re_2H_2$ structure **2H-3S** with C_s symmetry,

Table 8 Structures of $Cp_2Re_2H_6$ [=$Cp_2Re_2(\mu\text{-}H)_2H_4$] compared with the known $Cp^*_2Re_2H_6$ [=$Cp^*_2Re_2(\mu\text{-}H)_2H_4$]

6H-1S (C_{2h})	MPW1PW91	BP86	Experimental [6]
Re–Re (Å)	2.450	2.460	2.452
Cp(or Cp*)–Re (Å)	1.940	1.968	1.939
Re–H_{ter} (Å)	1.650	1.665	1.46(2), 1.63(3) (with the average 1.548)
Re–H_{bri} (Å)	1.796	1.812	1.87(2), 1.69(2) (with the average 1.782)
Re–Re–Cp (or Cp*) (°)	150.04	148.80	144.8
H_{ter}–Re–H_{ter} (°)	67.86	67.90	67(1)
Re–H_{bri}–Re (°)	86.00	85.47	86.6(9)

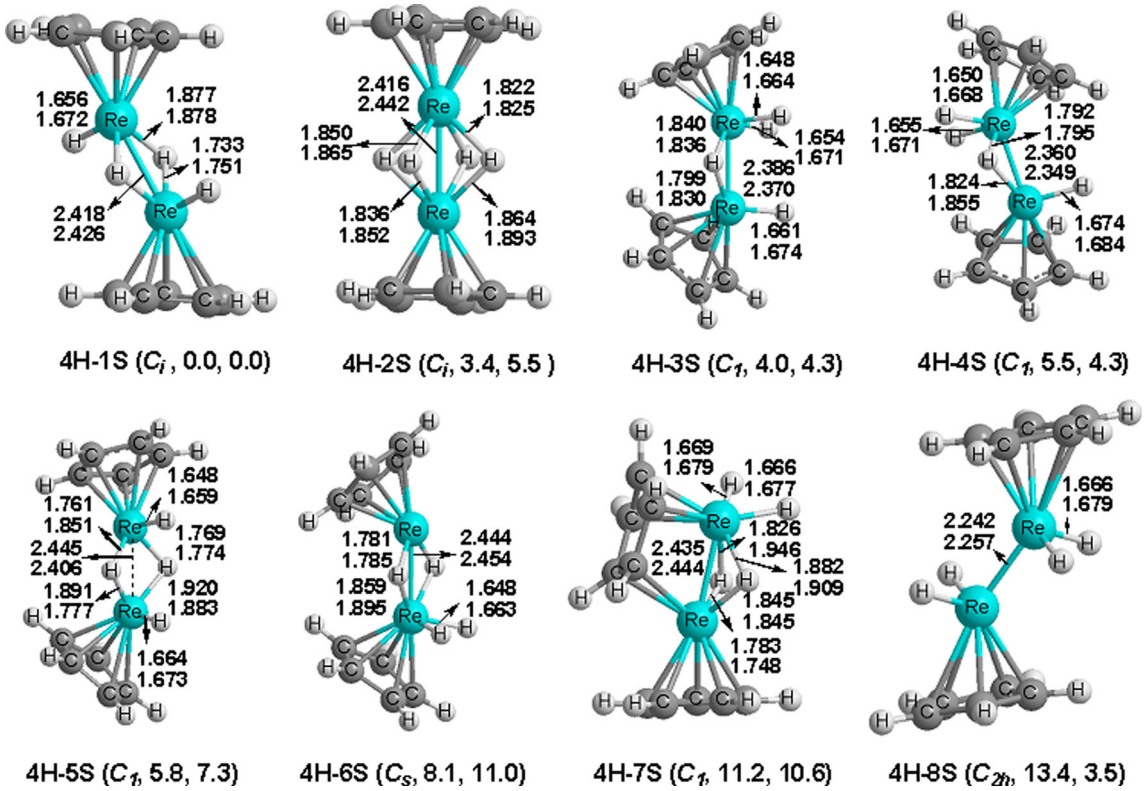

Fig. 5 The eight singlet stationary points of $Cp_2Re_2H_4$

lying 18.8 kcal mol^{-1} (MPW1PW91) or 17.9 kcal mol^{-1} (BP86) in energy above **2H-1S**, is geometrically similar to **2H-2S** except for *trans* rather than *cis* orientation of the terminal hydrogen atoms.

The next $Cp_2Re_2H_2$ structure **2H-4S**, lying 19.6 kcal mol^{-1} (MPW1PW91) or 22.2 kcal mol^{-1} (BP86) in energy above **2H-1S**, is predicted to be a bent C_s structure with two terminal η^5-Cp rings and two bridging hydrogen atoms (Fig. 6; Tables 11 and 12). The short bridging Re–H distances are 1.753 Å (MPW1PW91) or 1.781 Å (BP86) whereas the long bridging Re–H distances are 1.905 Å (MPW1PW91) or 1.849 Å (BP86). The short Re–Re distance of 2.376 Å (MPW1PW91) or 2.398 Å (BP86) in **2H-4S** can be considered to be a Re–Re single bond suggested by NBO analysis.

The last low-energy singlet $Cp_2Re_2H_2$ structure **2H-5S** (Fig. 6), lying 20.1 kcal mol^{-1} (MPW1PW91) or 20.9 kcal mol^{-1} (BP86) in energy above **2H-1S**, is predicted to be a bent C_2 structure with two terminal η^5-Cp rings in a *cis* orientation and a terminal hydrogen atom on each Re atom. The Re–H distances are 1.667 Å (MPW1PW91) or 1.678 Å

Table 9 Total energies (E, in Hartree), relative energies (ΔE, in kcal mol^{-1}), number of imaginary vibrational frequencies (Nimag) and Re–Re bond distance (Å) for the eight singlet state structures of $Cp_2Re_2H_4$

		4H-1S(C_i)	4H-2S(C_i)	4H-3S(C_1)	4H-4S(C_1)	4H-5S(C_1)	4H-6S(C_s)	4H-7S(C_1)	4H-8S(C_{2h})
MPW1PW91	E	−545.896019	−545.890674	−545.889643	−545.887239	−545.886759	−545.883065	−545.878229	−545.874658
	ΔE	0.0	3.4	4.0	5.5	5.8	8.1	11.2	13.4
	Nimag	0	1(22i)[a]	0	0	0	1(15i)[a]	0	0
	Re-Re	2.418	2.416	2.386	2.360	2.445	2.444	2.435	2.242
BP86	E	−546.182306	−546.173481	−546.175507	−546.175452	−546.170670	−546.164837	−546.165442	−546.176720
	ΔE	0.0	5.5	4.3	4.3	7.3	11.0	10.6	3.5
	Nimag	0	1(12i)[a]	0	0	0	1(24i)[b]	0	0
	Re-Re	2.426	2.442	2.370	2.349	2.406	2.454	2.444	2.257

[a] This imaginary vibrational frequency disappears using the finer (120 974) grid

[b] This imaginary vibrational frequency decreases to 1i cm^{-1} after using the finer (120 974) grid

Table 10 The ν(Re-H) frequencies (cm^{-1}) and IR intensities (km/mol^{-1}) for the eight $Cp_2Re_2H_4$ structures

	BP86
4H-1S (C_i)	1729(4)[a], 1733(0)[a], 2028(88), 2031(0)
4H-2S (C_i)	1541(0)[a], 1580(2)[a], 1597(2)[a], 1627(0)[a]
4H-3S (C_1)	1592(7)[a], 2031[a](44), 2044(27), 2067(35)
4H-4S (C_1)	1629(11)[a], 2005(79), 2033(28), 2038(40)
4H-5S (C_1)	1661(3)[a], 1686(27)[a], 2027(67), 2076(27)
4H-6S (C_s)	1663(5)[a], 1665(0)[a], 2046(13), 2058(60)
4H-7S (C_1)	1534(6)[a], 1788(10)[a], 1997(123), 2039(108)
4H-8S (C_{2h})	2029(0), 2031(81), 2040(80), 2044(0)

[a] Bridging ν(Re-H) frequencies

(BP86). The Re–Re distance is 2.274 Å (MPW1PW91) or 2.269 Å (BP86) in **2H-5S** can be interpreted as a formal triple bond suggested by the NBO analysis.

The hydride-free Cp_2Re_2 system

In a search for new metal–metal bonded systems with high order metal–metal multiple bonds, the Cp_2M_2 systems (M= Ta, W, Re, Os) were investigated in a previous study [7]. However, only structures with terminal η^5-Cp rings were found. The singlet Cp_2Re_2 structure of this type was found to have a short Re–Re distance. This was interpreted as a formal sextuple bond on the basis of the analysis of frontier molecular orbitals (FMOs).

A more extensive DFT study of the Cp_2Re_2 system has now been made, which included structures with bridging Cp rings as well as those with terminal Cp rings (Fig. 7, Table 13). Six energetically lower-lying Cp_2Re_2 structures were found, including structure **0H-4S** identical to the structure found in this previous work [7]. However, structure **0H-4S** was found to lie 38.3 kcal mol^{-1} (MPW1PW91) or 36.1 kcal mol^{-1} (BP86) above the lowest energy Cp_2Re_2 structure **0H-1S**. This suggests that the previously proposed Cp_2Re_2 structure with a formal metal–metal sextuple bond is of such high energy that it is never likely to be synthesized.

The global minimum singlet state Cp_2Re_2 structure **0H-1S** is predicted to be a C_{2v} perpendicular structure with two bridging η^2,η^3-Cp rings and with all real vibrational frequencies (Fig. 7, Table 13). The ultrashort Re–Re distance of 2.169 Å (MPW1PW91) or 2.195 Å (BP86), can be interpreted as a formal triple bond according to NBO analysis. This is consistent with a vacant coordination site on each Re atom *trans* to the Re–Re bond.

The next Cp_2Re_2 structure **0H-2S**, lying 15.1 kcal mol^{-1} (MPW1PW91) or 16.2 kcal mol^{-1} (BP86) in energy above **0H-1S**, is predicted to be a C_s structure with one terminal η^5-Cp ring and one bridging η^3,η^2-Cp ring (Fig. 7; Table 13).

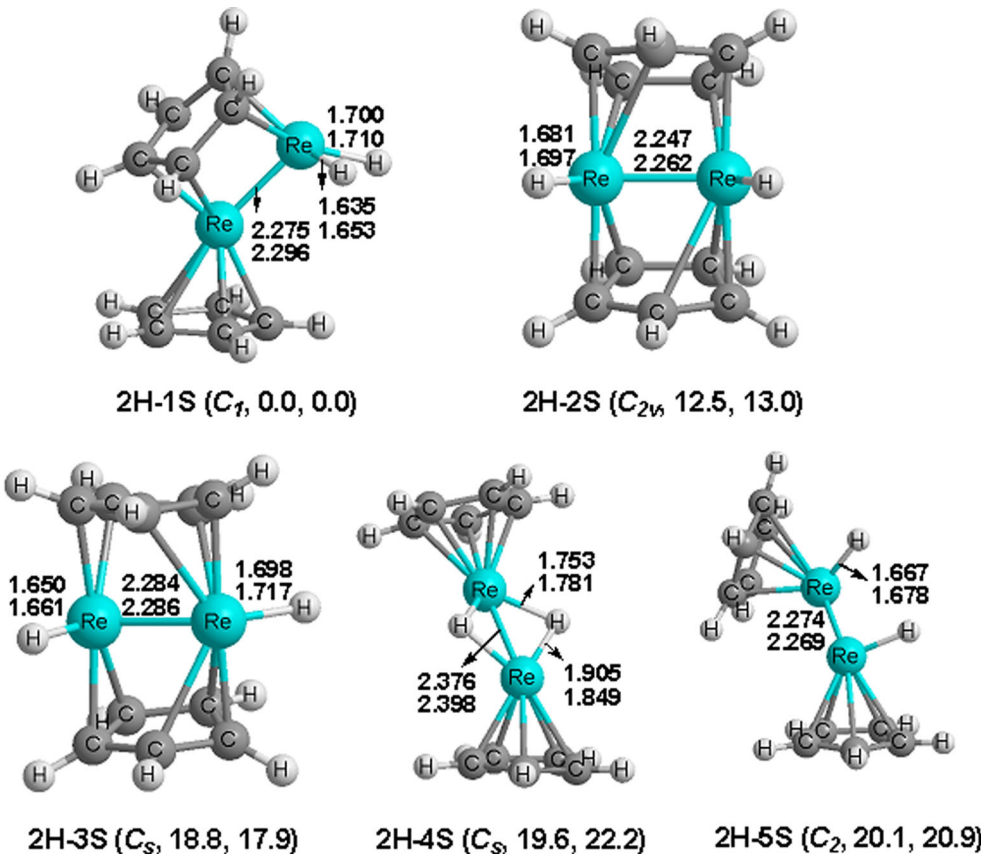

Fig. 6 The five singlet stationary points for $Cp_2Re_2H_2$

Table 11 Total energies (E, in Hartree), relative energies (ΔE, in kcal mol^{-1}), and Re-Re bond distance (Å) for the five singlet state structures of $Cp_2Re_2H_2$. None of these structures has any imaginary vibrational frequencies

		2H-1S (C_1)	2H-2S (C_{2v})	2H-3S (C_s)	2H-4S (C_s)	2H-5S (C_2)
MPW1PW91	E	−544.687877	−544.668019	−544.657953	−544.656571	−544.655842
	ΔE	0.0	12.5	18.8	19.6	20.1
	Nimag	0	0	0	0	0
	Re-Re	2.275	2.247	2.284	2.376	2.274
BP86	E	−544.980924	−544.960145	−544.952385	−544.945580	−544.947683
	ΔE	0.0	13.0	17.9	22.2	20.9
	Nimag	0	0	0	0	0
	Re-Re	2.296	2.262	2.286	2.398	2.269

The short Re–Re distance of 2.275 Å (MPW1PW91) or 2.297 Å (BP86) suggests a triple bond corresponding to the NBO analysis. Structure **0H-3S**, lying 23.7 kcal mol^{-1} (MPW1PW91) or 22.0 kcal mol^{-1} (BP86) in energy above **0H-1S**, is similar to **0H-2S** except for the bonding of the bridging η^3, η^2-Cp ring to the pair of Re atoms. Thus in **0H-3S**, the rhenium atom not bonded to the terminal η^5-Cp ring is bonded to three carbons of the bridging η^3,η^2-Cp ring rather than only two carbon atoms of the bridging η^3,η^2-Cp ring in **0H-2S**. Thus, structure **0H-3S** can be derived from **0H-2S** by rotation of the bridging Cp ring relative to a fixed CpRe-Re unit.

The next singlet Cp_2Re_2 structure **0H-4S** with two terminal η^5-Cp rings, lying ~37 kcal mol^{-1} in energy above **0H-1S** (Fig. 7, Table 13), is identical to the structure **Re-S** found by Xu et al. [7]. The predicted Re–Re distance of 2.247 Å (MPW1PW91) or 2.193 Å (BP86) in **0H-4S** is identical to that found by Xu et al. and has been suggested to indicate a formal sextuple bond by analysis of its FMOs. However, there is just a double bond between the two Re atoms in **0H-4S** by NBO analysis.

Two triplet Cp_2Re_2 structures were found (Fig. 7, Table 13). Structure **0H-1T**, lying 12.9 kcal mol^{-1} (MPW1PW91) or 20.0 kcal mol^{-1} (BP86) in energy (MPW1PW91) above **0H-1S**, is a perpendicular structure geometrically similar to **0H-1S**. The higher energy triplet Cp_2Re_2 structure **0H-2T**, lying 30.0 kcal mol^{-1} (MPW1PW91) or 35.1 kcal mol^{-1} (BP86) in energy above **0H-1S**, is identical to the structure Re-T_1 found by Xu et al. [7] with a Re–Re distance of 2.323 Å (MPW1PW91) or 2.272 Å (BP86) (Fig. 7, Table 13). Analysis of the FMOs in the previous work suggested a formal quintuple bond in **0H-2T**. However, there is a triple bond between the two Re atoms in **0H-2T** by NBO analysis.

Table 12 ν(Re-H) frequencies (cm^{-1}) and IR intensities (km mol^{-1}) for the five $Cp_2Re_2H_2$ structures

	BP86
2H-1S (C_1)	1918(197), 2077(112)
2H-2S (C_{2v})	1924(159), 1926(222)
2H-3S (C_s)	1844(265), 2059(124)
2H-4S (C_s)	1671(6)[a], 1677(7)[a]
2H-5S (C_2)	2017(11), 2024(99)

[a] Bridging ν(Re-H) frequencies

Thermochemistry

Table 14 lists the dissociation, disproportionation, and hydrogen dissociation energies of the cyclopentadienylrhenium hydrides, considering the lowest energy structures. The binuclear derivative $Cp_2Re_2H_8$ does not appear to be viable since its dissociation to $Cp_2Re_2H_6+H_2$ is slightly exothermic and spontaneous at −10.1 kcal mol^{-1} (MPW1PW91) or −13.8 kcal mol^{-1} (BP86). However, the energy required for further dissociation of H_2 from $Cp_2Re_2H_6$ to give $Cp_2Re_2H_4$ is substantial at 39.6 kcal mol^{-1} (MPW1PW91) or 35.2 kcal mol^{-1} (BP86), suggesting viability of $Cp_2Re_2H_6$. Hydrogen dissociation from the mononuclear $CpReH_6$ to give $CpReH_4$ is also highly endothermic requiring ~34 kcal mol^{-1}. The dimerization of $2CpReH_4$ to $Cp_2Re_2H_8$ is a highly exothermic process with a predicted energy release of ~56 kcal mol^{-1}. This predicted thermochemistry of the cyclopentadienylrhenium hydrides is consistent with the experimental observation that the pentamethylcyclopentadienyl derivatives Cp^*ReH_6 and $Cp^*_2Re_2H_6$ have been synthesized as stable compounds [4–6].

The nature of Re–Re multiple bonds in $Cp_2Re_2H_n$ (n=0, 2, 4, 6, 8)

Table 15 lists the Wiberg bond indices (WBIs), Re–Re distances, formal bond orders, and bridging groups atomic from NBO analysis [21, 22] of $Cp_2Re_2H_n$ (n=8, 6, 4, 2, 0) using the MPW1PW91 method. Previous studies [37] on the WBIs of metal carbonyls such as $Fe_2(CO)_9$ and $Fe_3(CO)_{12}$ show that the WBIs are relatively low compared with the formal bond orders, particularly when the metal–metal bonds are bridged by carbonyl groups.

Examination of the data presented in Table 15 shows that the WBIs depend not only on the formal Re–Re bond order but also the groups bridging the Re–Re bond. However, in general, the WBIs are consistent with the bond orders suggested by the Re–Re distances and

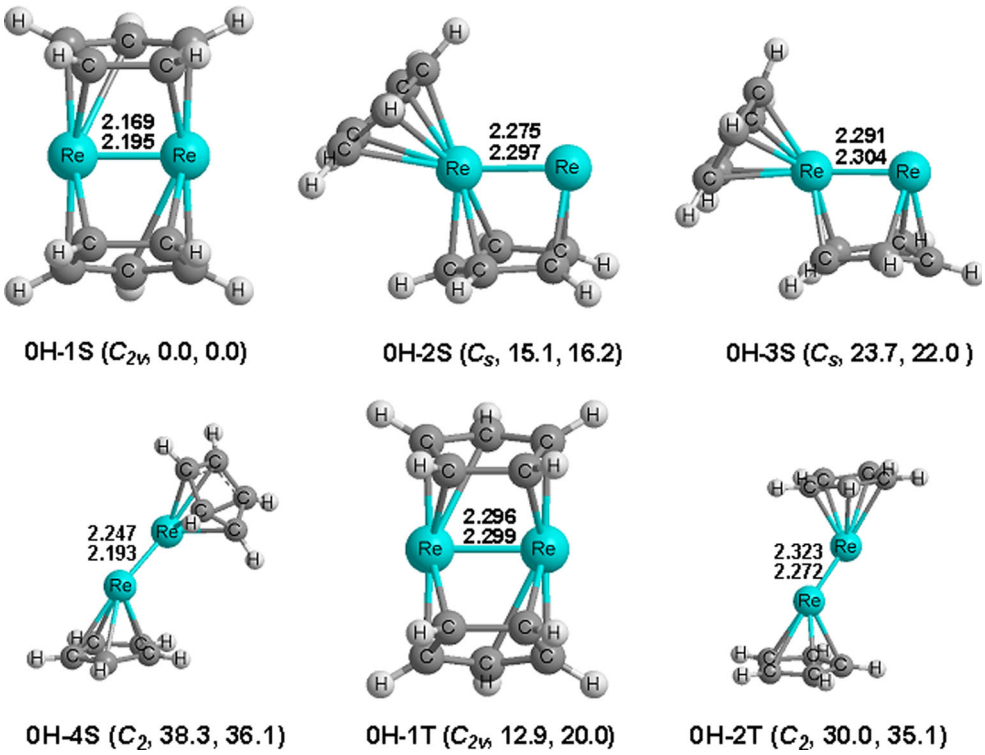

Fig. 7 The four singlet and two triplet stationary points of Cp_2Re_2

electron counting. For the unbridged structures without the complication of bridging groups, the WBIs for formal triple, and quadruple bonds are ~2.1–2.5 and ~2.7, respectively. The previous suggestion of a formal Re–Re sextuple bond in the previously found [7] Cp_2Re_2 structure **0H-4S** based on FMO analysis is supported by its abnormally high Re–Re WBI of ~3.47, which is more than ~1 greater than any of the other WBIs found in this work.

The presence of bridging groups in the $Cp_2Re_2H_n$ structures can lower the WBIs and increase the Re–Re distances significantly for a given formal Re–Re bond order. This is a clear consequence of orbitals from the bridging groups interacting with two-center two-electron components of the Re–Re bonds, thereby making them three-center two-electron bonds and thus weakening the Re–Re interactions for a given formal bond order. Thus, for the $Cp_2Re_2H_6$ structures **6H-3S** and **6H-4S**, the unbridged formal Re≡Re triple bond has a WBI of ~2.1 with a length of ~2.29 Å. However, bridging the Re≡Re triple bond with two hydrogen atoms in **6H-1S** and **6H-2S** lowers the WBI to ~1.4 and lengthens the Re–Re bond to ~2.46 Å. For formal Re–Re bonds in $Cp_2Re_2H_4$, the structures with no bridging hydrogen atoms, two bridging hydrogen atoms, and four bridging hydrogen atoms have WBIs of ~2.6, ~1.7, and ~1.6, respectively, regarded as quadruple bonds, double bonds and single bonds by NBO analysis with

Table 13 Total energies (E, in hartree), relative energies (ΔE, in kcal/mol^{-1}), numbers of imaginary vibrational frequencies (Nimag) and Re–Re bond distances (Å) for the five singlet state and two triplet spin state Cp_2Re_2 structures of Cp_2Re_2

		0H-1S(C_{2v})	0H-2S(C_s)	0H-3S(C_s)	0H-4S(C_2)	0H-1T(C_{2v})	0H-2T(C_2)
MPW1PW91	E	−543.458445	−543.434349	−543.420624	−543.397466	−543.437829	−543.410657
	ΔE	0.0	15.1	23.7	38.3	12.9	30.0
	Nimag	0	0	0	0	0	0
	Re-Re	2.169	2.275	2.291	2.247	2.296	2.323
BP86	E	−543.754633	−543.728763	−543.719639	−543.697166	−543.722799	−543.698712
	ΔE	0.0	16.2	22.0	36.1	20.0	35.1
	Nimag	0	0	0	0	0	1(18i)[a]
	Re-Re	2.195	2.297	2.304	2.193	2.299	2.272

[a] This imaginary vibrational frequency disappears using the finer (120,974) grid

Table 14 Predicted thermochemistry of $CpReH_n$ and $Cp_2Re_2H_n$ derivatives

	ΔG	
	MPW1PW91	BP86
$Cp_2Re_2H_8 \rightarrow Cp_2Re_2H_6+H_2$	−10.1	−13.8
$Cp_2Re_2H_6 \rightarrow Cp_2Re_2H_4+H_2$	39.6	35.2
$Cp_2Re_2H_4 \rightarrow Cp_2Re_2H_2+H_2$	22.5	16.4
$Cp_2Re_2H_2 \rightarrow Cp_2Re_2+H_2$	36.9	33.0
$Cp_2Re_2H_8 \rightarrow CpReH_2+ CpReH_6$	55.5	53.1
$Cp_2Re_2H_6 \rightarrow CpReH_2+ CpReH_4$	99.8	101.7
$CpReH_6 \rightarrow CpReH_4+H_2$	34.2	34.8
$CpReH_4 \rightarrow CpReH_2+H_2$	33.7	34.4
$CpReH_2 \rightarrow CpRe+H_2$	36.6	38.2
$2CpReH_6 \rightarrow Cp_2Re_2H_8+2H_2$	12.4	16.1
$2CpReH_6 \rightarrow Cp_2Re_2H_6+3H_2$	2.3	2.3
$2CpReH_6 \rightarrow Cp_2Re_2H_4+4H_2$	41.9	37.5
$2CpReH_6 \rightarrow Cp_2Re_2H_2+ 5H_2$	64.4	53.8
$2CpReH_6 \rightarrow Cp_2Re_2+6H_2$	101.3	86.9
$2CpReH_4 \rightarrow Cp_2Re_2H_8$	−56.0	−53.6
$2CpReH_4 \rightarrow Cp_2Re_2H_6+H_2$	−66.0	−67.4
$2CpReH_4 \rightarrow Cp_2Re_2H_4+2H_2$	−26.5	−32.2
$2CpReH_4 \rightarrow Cp_2Re_2H_2+3H_2$	−4.0	−15.8
$2CpReH_4 \rightarrow Cp_2Re_2+4H_2$	32.9	17.2
$2CpReH_2 \rightarrow Cp_2Re_2H_4$	−94.0	−100.9
$2CpReH_2 \rightarrow Cp_2Re_2H_2+H_2$	−71.5	−84.6
$2CpReH_2 \rightarrow Cp_2Re_2+2H_2$	−34.6	−51.5

Re–Re distances of ~2.24 Å, ~2.40 Å, and ~2.42 Å, respectively.

Figure 8 shows the NBOCMO bonding molecular orbitals only for the Re≡Re triple bond and Re≡Re quadruple bond. As expected (and seen in Fig. 8), the Re≡Re triple bond in **6H-3S** consists of one formal σ-bond and two-π bond molecular orbitals. And the two π bond molecular orbitals are mainly from the contribution of d orbitals. It is worth mentioning that the σ-bond in **6H-3S** contains the contribution of 25.47 % from the s orbital and the others from the d orbitals. Interestingly, the σ-bond in **6H-4S** also has a contribution of 26.44 % from the s orbital. This indicates that the σ-bond between the metal atoms may mix a part of the s orbital contribution. The only quadruple metal–metal bond found in **4H-8S** consists of one σ-bond molecular orbital, two π-bond molecular orbitals and one δ-bond molecular orbital. Thus, the two π-bond molecular orbitals and the δ-bond molecular orbital are certainly derived mainly from the d orbitals, while the σ-bond molecular orbital mixes the s orbital character to a larger percentage at 29.77 %. Re≡Re triple bonds were also found in **2H-5S**, **0H-1S**, **0H-2S** and **0H-3S**.

Table 15 Wiberg bond indices (WBI) of Re–Re bonds, Re–Re bond distances and the bond order by GenNBO analysis in the structures of $Cp_2Re_2H_n$ (n=0,2, 4, 6, 8) calculated at the MPW1PW91/DZP level of theory

	MPW1PW91(Re-Re)			
	WBI	Bond length(Å)	Bond order	Bridging groups
0H-1S(C_{2v})	2.67	2.169	3	2Cp
0H-2S(C_s)	2.58	2.275	3	Cp
0H-3S(C_s)	2.59	2.291	3	Cp
0H-4S(C_2)	3.47	2.246	2	None
0H-1T(C_{2v})	1.73	2.296	2	2Cp
0H-2T(C_2)	2.40	2.323	3	None
2H-1S(C_1)	2.31	2.275	2	Cp
2H-2S(C_{2v})	1.91	2.247	2	2Cp
2H-3S(C_s)	1.90	2.284	2	2Cp
2H-4S(C_s)	2.16	2.376	1	2H
2H-5S(C_2)	2.46	2.274	3	None
4H-1S(C_i)	1.71	2.418	2	2H
4H-2S(C_i)	1.58	2.416	1	4H
4H-3S(C_1)	1.65	2.386	2	H
4H-4S(C_1)	1.86	2.360	2	H
4H-5S(C_1)	1.31	2.445	0	2H
4H-6S(C_s)	1.45	2.444	1	2H
4H-7S(C_1)	1.28	2.435	1	2H
4H-8S(C_{2h})	2.62	2.242	4	None
6H-1S(C_{2h})	1.40	2.450	1	2H
6H-2S(C_{2v})	1.35	2.466	1	2H
6H-3S(C_{2h})	2.11	2.291	3	None
6H-4S(C_2)	2.09	2.297	3	None
8H-1S(C_{2h})	0.58	2.769	0	2H
8H-2S(C_{2v})	0.51	2.839	0	2H
8H-3S(C_{2h})	1.28	2.580	2	None

In order to further ascertain the existence of the quadruple rhenium–rhenium bond in **4H-8S**, the electron density ρ(r) values at the (3, −1) bond critical points of the Re–Re bond were obtained as well as the Re–Re quadruple bond in dianion [36] $Re_2Cl_8^{2-}$ using AIM (atoms in molecules) [39] analysis (Fig. 9). Interestingly, there is a significant larger electron density of 0.169 e/bohr^3 at the Re–Re BCP in dianion $Re_2Cl_8^{2-}$. And the electron density of 0.165 e/bohr^3 at the Re–Re BCP in **4H-8S** is as large as the electron density at the Re–Re BCP in dianion $Re_2Cl_8^{2-}$. This indicates the existence of a Re≡Re quadruple bond between the two Re atoms in **4H-8S**.

Figure 10 shows the calculated overlap population density-of-state (OPDOS [24, 25]) between three molecular fragments. DFT calculations reveal that the Re–Re bonding interaction resides in the HOMO to HOMO-3 relating to the

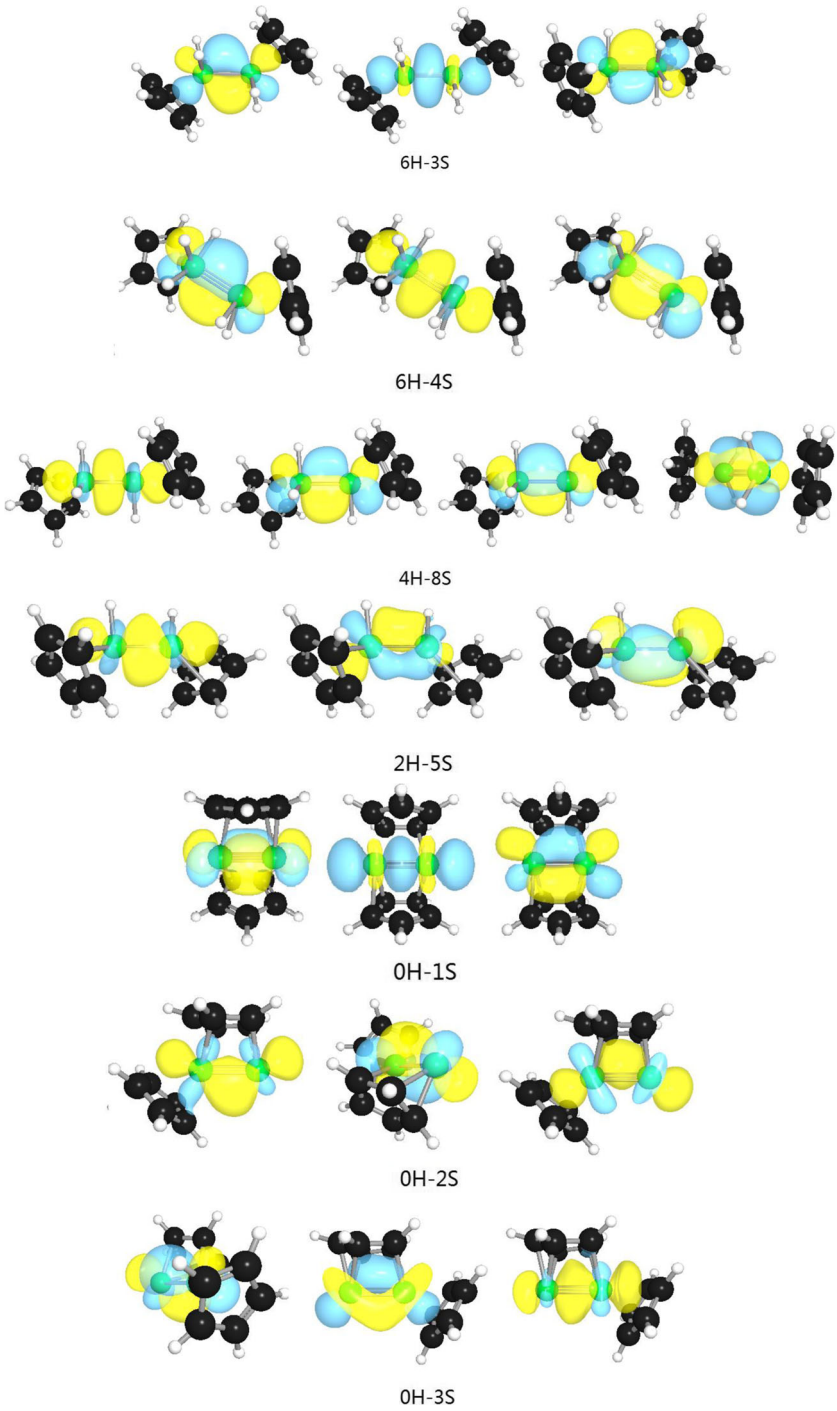

Fig. 8 Canonical molecular orbitals (CMO) of the Re–Re bonding molecular orbitals generated with NBOview [38]

rhenium–rhenium bonding with an isosurface contour value of 0.05. The molecular orbital energies of HOMO-2 and HOMO-1 are −6.59 eV and −6.33 eV, respectively, indicating they are the degenerate states. Thus, the two molecular orbital are on the same peak. The HOMO to HOMO-3 clearly have a positive overlap population between the Re atoms, indicating the presence of the Re≡Re quadruple bond in **4H-8S**.

Discussion

The lowest energy $Cp_2Re_2H_n$ structures (n=8, 6, 4) all have terminal Cp rings and a Re–Re bond bridged by two hydrogen atoms. The permethylated $Cp^*_2Re_2H_6$ structure of this type is known experimentally [6], having been synthesized by photolysis or pyrolysis of Cp^*ReH_6. $Cp_2Re_2H_n$ structures (n=8, 6, 4) with exclusively terminal hydrogen atoms are also found at

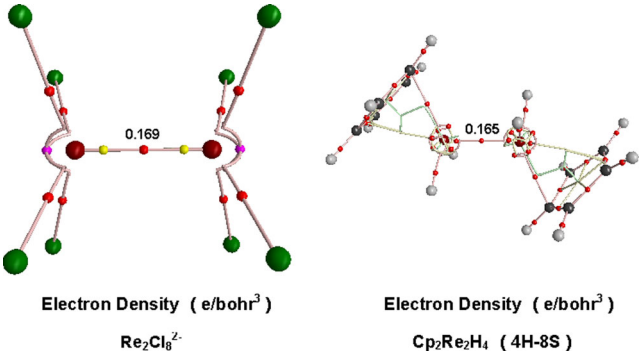

Fig. 9 Selected electron densities at the (3, −1) bond critical points of the Re–Re bond shown in *red* calculated by atoms in molecules (AIM) analysis using the density functional theory (DFT)-optimized structure $Re_2Cl_8^{2-}$ and $Cp_2Re_2H_4$ (**4H-8S**) at MPW1PW91/DZP level

accessible but significantly higher energies than their doubly bridged isomers.

The $Cp_2Re_2H_4$ system has the most complicated potential energy surface of the $Cp_2Re_2H_n$ systems with eight structures within 14 kcal mol^{-1} of the lowest energy structure **4H-1S**. These structures exhibit some interesting features. Thus the tetrabridged $Cp_2Re_2(\mu\text{-H})_4$ structure **4H-2S**, lying only ~4 kcal mol^{-1} above **4H-1S**, is a rare example of a tetrabridged binuclear transition metal structure that is a genuine minimum without large imaginary vibrational frequencies. The unsymmetrical singly bridged $Cp_2Re_2(\mu\text{-H})H_3$ structures **4S-3S** and **4H-4S** are also energetically accessible, lying only ~5 kcal mol^{-1} above **4H-1S**. A bridging Cp ring is found in the somewhat higher energy $Cp(\mu\text{-Cp})Re(\mu\text{-H})_2H_2$ structure **4H-7S**, lying ~11 kcal mol^{-1} above **4H-1S**.

The lowest energy $Cp_2Re_2H_2$ structure **2H-1S** is a $Cp(\mu\text{-Cp})ReH_2$ structure similar to **4H-7S** with a bridging and a terminal Cp ring. Structure **2H-1S** can be derived from **4H-7S** by removal of the two bridging hydrogen atoms. This $Cp(\mu\text{-Cp})ReH_2$ structure appears to be a very favorable structure, since the next highest energy $Cp_2Re_2H_2$ structure **2H-2S** is predicted to lie ~13 kcal mol^{-1} above **2H-1S**. Structure **2H-2S** is a perpendicular $(\mu\text{-Cp})_2Re_2H_2$ structure with two parallel bridging Cp rings and a terminal hydrogen bonded to each rhenium atom. This is the hydrogen-richest perpendicular $(\mu\text{-Cp})_2Re_2H_n$ structure found in this work. Apparently perpendicular $(\mu\text{-Cp})_2M_2L_n$ structures become unfavorable when there are too many external ligands L outside the central $(\mu\text{-Cp})_2M_2$ unit.

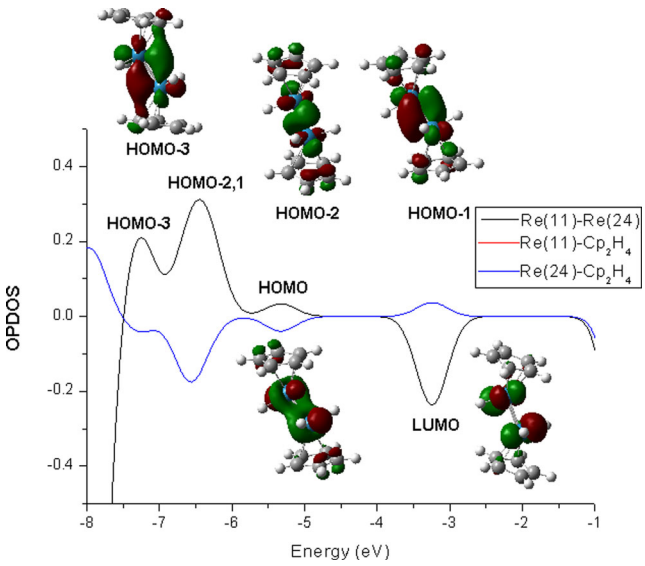

Fig. 10 Calculated overlap population density of states (OPDOS) for $Cp_2Re_2H_4$ (4H-8S) explored by AOMIX [24, 25]. *Insets* 3D representations of the HOMO to HOMO-3 and LUMO. The former clearly have positive overlap population between the Re atoms

A higher energy unbridged $Cp_2Re_2H_4$ structure **4H-8S** is suggested containing the only formal Re–Re quadruple bond required to give each rhenium atom the favored 18-electron configuration. NBOCMO analysis, AIM and OPDOS in AOMIX all also indicate the existence of the quadruple bond.

A previous study on the hydride-free Cp_2Re_2 system led to the bent singlet and triplet Cp_2Re_2 structures (**0H-4S** and **0H-2T**, respectively) with terminal Cp rings and short M–M distances [7]. These structures were suggested to have formal sextuple and quintuple Re–Re bonds, respectively, on the basis of FMO analysis. The same structures were also found in this work but at energies more than 30 kcal mol^{-1} above the lowest energy Cp_2Re_2 structure **0H-1S**.

In order to gain some insight into the thermochemistry of the cyclopentadienylrhenium hydride system, the mononuclear $CpReH_n$ derivatives (n=6, 4, 2) were also included in this study. The predicted $CpReH_6$ structure including the Re–H distances is close to the experimental structure for the very stable, experimentally known, Cp*ReH_6. The predicted high energy of ~34 kcal mol^{-1} required for H_2 elimination from $CpReH_6$ to give $CpReH_4$ is consistent with the high stability of Cp*ReH_6. For the binuclear derivatives the slightly exothermic H_2 dissociation of ~10.1 kcal mol^{-1} from $Cp_2Re_2H_8$ to give $Cp_2Re_2H_6$ suggests that $Cp_2Re_2H_8$ is not a viable species. On the other hand the relatively high energy of ~39.6 kcal mol^{-1} required for H_2 dissociation from $Cp_2Re_2H_6$ to give $Cp_2Re_2H_4$ is consistent with the synthesis of $Cp^*_2Re_2H_6$ as a stable compound. In addition, the previously reported [7] bent triplet and singlet Cp_2Re_2 structures with terminal Cp rings suggested to have formal quintuple and sextuple Re–Re bonds do not appear to be promising synthetic objectives. Alternative perpendicular Cp_2Re_2 structures with bridging Cp rings lie more than 30 kcal mol^{-1} below these previously reported structures and are likely to be the products of a successful synthesis of a Cp_2Re_2 molecule. Such synthesis might, for example, arise from

the dehalogenation of a cyclopentadienylrhenium halide, such as the known [40] Cp^*ReCl_4.

Conclusions

The lowest energy structures of the binuclear cyclopentadienylrhenium hydrides $Cp_2Re_2H_n$ (n=4, 6, 8) have a central doubly bridged $Re_2(\mu\text{-}H)_2$ with terminal η^5-Cp rings and the remaining hydrides as terminal ligands. However, the lowest $Cp_2Re_2H_2$ structure by more than 12 kcal mol^{-1} has one terminal η^5-Cp ring, a bridging η^3,η^2-Cp ring, and two terminal hydride ligands bonded to the same Re atom. The lowest energy hydride-free Cp_2Re_2 structure is a perpendicular structure with two bridging η^3,η^2-Cp rings. The previously predicted bent singlet Cp_2Re_2 structure with terminal η^5-Cp rings and a formal Re-Re sextuple bond lies ~37 kcal mol^{-1} above this lowest energy $(\eta^3,\eta^2\text{-Cp})_2Re_2$ structure and thus is unlikely to be synthesized.

A higher energy unbridged $Cp_2Re_2H_4$ structure **4H-8S** is suggested containing the only formal Re Re quadruple bond required to give each rhenium atom the favored 18-electron configuration. NBOCMO analysis, AIM and OPDOS in AOMIX all also indicate the existence of the quadruple bond, which is the highest rhenium–rhenium bond order found in this work.

The thermochemistry of the $CpReH_n$ and $Cp_2Re_2H_n$ systems is consistent with the experimental observation of the very stable permethylated derivatives [4, 5] Cp^*ReH_6 and $Cp^*_2Re_2H_6$ [6]. Thus the predicted H_2 dissociation energies from $CpReH_6$ to give $CpReH_4$ and from $Cp_2Re_2H_6$ to give $Cp_2Re_2H_4$ are relatively high at ~39.6 kcal mol^{-1}. However, H_2 dissociation from $Cp_2Re_2H_8$ to give $Cp_2Re_2H_6$ is predicted to be slightly exothermic at ~10.1 kcal mol^{-1}.

Acknowledgments We are indebted to the Excellent Young Scholars Research Fund of Beijing Institute of Technology (2012YG0202 and 2014CX04024), Beijing Natural Science Foundation (2132033, and 2132035), Beijing Higher Education Young Elite Teacher Project(YETP1177) and the National Natural Science Foundation of China (61440020) and the U.S. National Science Foundation (Grants CHE-1057466 and CHE-1054286) for support of this research.

References

1. Lundell GEF, Knowles HB (1937) J Res Natl Bur Std 18:629–637
2. Abrahams AC, Ginsberg AP, Knox K (1964) Inorg Chem 3:558–567
3. Green MLH, Pratt L, Wilkinson G (1958) J Chem Soc 3916–3922
4. Herrmann WA, Okuda J (1986) Angew Chem Int Ed 25:1092–1093
5. Herrmann WA, Theiler HG, Kiprof P, Tremmel J, Blom R (1990) J Organometal Chem 395:69–84
6. Herrmann WA, Theiler HG, Eberhardt H, Paul K (1989) J Organometal Chem 367:291–311
7. Xu B, Li QS, Xie YM, King RB, Schaefer HF (2010) J Chem Theory Comput 6:735–746
8. Frisch MJ, Trucks GW, Schlegel HB, Scuseria GE, Robb MA, Cheeseman JR, Scalmani G, Barone V, Mennucci B, Petersson GA, Nakatsuji H, Caricato M, Li X, Hratchian HP, Izmaylov AF, Bloino J, Zheng G, Sonnenberg JL, Hada M, Ehara M, Toyota K, Fukuda R, Hasegawa J, Ishida M, Nakajima T, Honda Y, Kitao O, Nakai H, Vreven T, Montgomery JA Jr, Peralta JE, Ogliaro F, Bearpark M, Heyd JJ, Brothers E, Kudin KN, Staroverov VN, Kobayashi R, Normand J, Raghavachari K, Rendell A, Burant JC, Iyengar SS, Tomasi J, Cossi M, Rega N, Millam JM, Klene M, Knox JE, Cross JB, Bakken V, Adamo C, Jaramillo J, Gomperts R, Stratmann RE, Yazyev O, Austin AJ, Cammi R, Pomelli C, Ochterski JW, Martin RL, Morokuma K, Zakrzewski VG, Voth GA, Salvador P, Dannenberg JJ, Dapprich S, Daniels AD, Farkas Ö, Foresman JB, Ortiz JV, Cioslowski J, Fox DJ (2009) Gaussian 09, revision A.1. Gaussian, Inc, Wallingford
9. Becke AD (1988) Phys Rev A 38:3098–3100
10. Perdew JP (1986) Phys Rev B 33:8822–8824
11. Adamo C, Barone V (1998) J Chem Phys 108:664–675
12. Zhao Y, Pu J, Lynch BJ, Truhlar DG (2004) Phys Chem Chem Phys 6:673–676
13. Perdew JP (1991) In: Ziesche P, Esching H (eds) Electronic structure of solids. Akademic, Berlin, p 11
14. Zhao S, Wang W, Li Z, Liu ZP, Fan KN, Xie YM, Schaefer HF (2006) J Chem Phys 124:184102
15. Feng X, Gu J, Xie YM, King RB, Schaefer HF (2007) J Chem Theory Comput 3:1580–1587
16. Andrae D, Häußermann U, Dolg M, Stoll H, Preuß H (1990) Theor Chim Acta 77:123–141
17. Dunning TH (1970) J Chem Phys 53:2823–2833
18. Huzinaga S (1965) J Chem Phys 42:1293–1302
19. Leininger ML, Huis TJV, Schaefer HF (1997) J Phys Chem A 101: 4460–4464
20. Papas BN, Schaefer HF (2006) J Mol Struct Theochem 768:175–181
21. Glendening ED, Badenhoop JK, Reed AE, Carpenter JE, Bohmann JA, Morales CM, Weinhold F (2001) NBO 5.0. Theoretical Chemistry Institute, University of Wisconsin-Madison, Madison
22. Weinhold F, Landis CR (2005) Valency and bonding: a natural bond order donor-acceptor perspective. Cambridge University Press, Cambridge, pp 32–36
23. König FB, Schönbohm J, Bayles D (2001) AIM2000—a program to analyze and visualize atoms in molecules. J Comput Chem 22:545–559
24. Gorelsky SI, AOMix program, rev. 5.62. http://www.obbligato.com/software/aomix
25. Gorelsky SI, Lever ABP (2001) J Organomet Chem 635:187–196
26. Herrmann WA, Flöel M, Kulpe J, Felixberger JK, Herdtweck E (1988) J Organometal Chem 355:297–313
27. Bau R, Carroll WE, Teller RG (1977) J Am Chem Soc 99:3872–3874
28. Hinman JG, Rashid KA, Lough AJ, Morris RH (2001) Inorg Chem 40:2480–2481
29. Michael TC, Phillip EF, Mark AG, Richard AW (1992) Inorg Chem 31:2359–2365
30. Abrahams SC, Ginsberg AP, Koetzle TF, Marsh P, Sprinkle CR (1986) Inorg Chem 25:2500–2510
31. Green MA, Huffman JC, Caulton KG (1982) J Am Chem Soc 104: 2319–2320
32. Wang CZ, Zhang XH, Li QS, Xie YM, King RB, Schaefer HF (2012) J Mol Model 18:2387–2398
33. Shima T, Suzuki H (2005) Organometallics 24:3939–3945
34. Ohki Y, Suzuki H (2000) Angew Chem Int Ed 39:3120–3122
35. Koga N, Morokuma K (1993) J Mol Struct 300:181–189
36. Cotton FA, Harris CB (1965) Inorg Chem 4:330–333

37. Wang H, Xie Y, King RB, Schaefer HF (2006) J Am Chem Soc 128: 11376–11384
38. Wendt M, Weinhold F (2001) NBOView 1.1. Theoretical Chemistry Institute, University of Wisconsin-Madison, Madison
39. Richard DA, Yuan OW, Zhang Q (2013) Organometallics 32:7540–7546
40. Herrmann WA, Herdtwick E, Floel M, Kulpe J, Kusthardt U, Okuda J (1987) Polyhedron 6:1165–1182